

Photoluminescence Spectroscopy of Cadmium Telluride Deep Defects

Paul J. Roland, Naba R. Paudel, Chuanxiao Xiao, Yanfa Yan, Randy J. Ellingson

Department of Physics & Astronomy, University of Toledo, Toledo, OH, 43606 USA

Abstract — Deep defect states of Cadmium Telluride deposited via close space sublimation and magnetron sputtering are evaluated via steady state and time resolved photoluminescence. Intensity dependent photoluminescence measurements for as-grown and cadmium chloride treated samples reveal the recombination mechanism associated with each transition. The as-grown sputtered film photoluminescence is weak with broad features while the close space sublimation film photoluminescence is comparatively bright and dominated by a deep donor acceptor pair recombination. Unlike excitonic or free-to-bound transitions, donor acceptor pair recombination exhibits a distance dependence that determines the distribution of transition energies and recombination rates. We measure the PL lifetime with respect to energy as a direct observation of the increasing donor acceptor pair recombination rate with decreasing donor-acceptor separation.

Index Terms — cadmium telluride, defects, photoluminescence, carrier lifetime, donor acceptor pair

I. INTRODUCTION

Cadmium telluride (CdTe) is one of the most promising absorber materials for thin film photovoltaics. Polycrystalline CdTe thin films deposited via close space sublimation (CSS) have a record efficiency of 19.6% [1] despite the low temperature/low vacuum environment while the record efficiency as been recently set at 20.4% by First Solar, Inc. (deposition method not mentioned in press release) [2]. Sputtered CdTe films are typically deposited under higher temperature/higher vacuum and would be expected to yield higher quality films but result in lower efficiency devices, around 14.5% [3]. We are aware of only one previous publication comparing the luminescence of CSS and sputtered CdTe in which Moutinho et. al [4] reported that the cathodoluminescence spectra from CSS, physical vapor deposition, and sputtered CdTe were qualitatively similar. In order to better understand differences between devices made via CSS and sputtering, it is necessary to probe the defect states in the CdTe thin films. Here we present a detailed study of the CdTe defects in CSS and sputtered films via steady-state photoluminescence (PL) and time resolved photoluminescence (TRPL).

PL studies have revealed much over the years about the energy levels of various defect state [5]-[18] in CdTe including a 1.59 eV excitonic transition, 1.55 eV double peak “DP” band, 1.45 eV “A” band associated with a donor acceptor complex [5], and a 1.18 eV donor acceptor pair (DAP) [15]. Additionally, we show direct observation of the increased recombination rate of DAPs with decreasing

separation via TRPL measurements conducted at different energies.

II. SAMPLE PREPARATION

For samples of both CSS and sputtering deposition methods, CdTe films of two different thicknesses (2 μm and 4 μm) were deposited onto commercially available $\text{SnO}_2/\text{SnO}_2:\text{F}$ coated soda-lime glass substrate [TEC15] supplied by Pilkington, NA. The thin film samples were grown on a home built close-spaced sublimation (CSS) system using 99.999% (5N) purity CdTe powders purchased from Materion [19]. During the sublimation, the glass substrate was held at 540 $^\circ\text{C}$ and 50 Torr in 1% oxygen mixed helium ambient. For desired thicknesses, CSS deposition proceeded for 10 and 20 minutes respectively. For comparative study, a second set of samples with similar thicknesses were grown by magnetron sputtering using previously optimized parameters: 270 $^\circ\text{C}$ substrate temperature, 10 mTorr argon pressure and 50 W RF power [20]. In order to observe the effects caused by CdCl_2 activation, all CdTe samples were divided into two halves. One piece of each sample type was activated via the application of saturated solution of CdCl_2 powder and methanol, followed by heat treatment at 390 $^\circ\text{C}$ for 30 minutes in dry air.

II. PHOTOLUMINESCENCE

Samples were mounted in an Advanced Research Systems closed cycle He cryostat, and PL was measured using a Horiba iHR320 monochromator, Symphony II Si CCD or LN_2 cooled Ge detector, depending on photon energy. Steady-state PL measurements were conducted under 632 nm excitation while the laser intensity was varied from 0.74 to 10.5 mW/cm^2 to verify the type of each defect present by fitting the PL peak intensity to:

$$I_{PL} = I_{Laser}^k \quad (1)$$

The parameter k varies from 1 to 2 for band edge emission, and is less than 1 for free-to-bound or DAP transitions. DAP transitions can also be identified by their shift to higher energy with increasing photogenerated carrier density. As-grown and CdCl_2 treated CSS film spectra are depicted in Fig. 1 and exhibit multiple defect peaks (CdTe film thickness influenced the total PL intensity, but not which PL peaks were present).

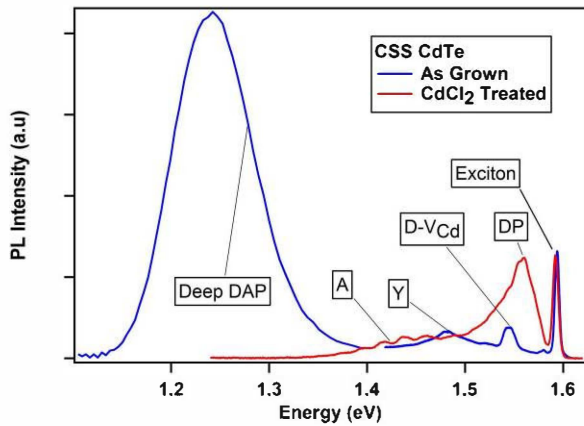


Fig. 1 PL spectra of CSS deposited CdTe before (blue curve) and after CdCl₂ treatment (red curve) under 1.2 mW/cm² illumination.

A. CSS Thin Film Photoluminescence

Fig. 1 shows the PL spectra for the as-grown and CdCl₂ treated CdTe films deposited via CSS. The as-grown sample consists of three peaks at 1.593 eV (D,X), 1.54 eV (D-V_{Cd}), 1.47 eV (Y band), and 1.25 eV (DAP). The CdCl₂ treated film however, shows transitions at 1.591 eV (A,X), 1.55 eV (DP), and a 1.45 eV (A Band) transition with phonon replica. Numerous authors [8, 9, 10, 15, 18] have reported exciton transitions due to donor-bound excitons (1.596 eV and 1.593 eV) and acceptor-bound excitons (1.591 eV and 1.587 eV). After CdCl₂ treatment, the exciton emission shifts from a donor-bound exciton to an acceptor-bound exciton, consistent with literature [15, 18]. The 1.55 eV transition consists of a double peak, labeled DP [18], and has been shown to be composed of a 1.552 eV DAP transition and a 1.559 eV free-to-bound transition involving an acceptor. The DAP consists of a shallow donor ($E_D = 8$ meV) while the two transitions utilize the same acceptor (near $E_A = 47$ meV) [12, 14, 18]. The 1.54-1.55 eV transition has been proposed to be a DAP transition involving a cadmium vacancy (D-V_{Cd}) [11].

The 1.47 eV Y band has been attributed to structural extended defect [10, 14, 18]; which coincides with the quenching of the Y band upon CdCl₂ treatment. The A band consists of a zero phonon line at 1.457 eV with multiple phonon replica separated by 21 meV, consistent with the LO phonon for CdTe [5, 8, 9, 14, 15, 18] and has been linked to the (V_{Cd},Cl_{Te}) acceptor complex. Corwine et. al [13] propose, instead, that the 1.45 eV peak requires the presence of both copper and oxygen instead of intrinsic defects. As our experiments lack any doping control, we are unable to offer an opinion as to which is correct. Finally, the deep defect observed at 1.25 eV in Fig. 1 is related to a DAP transition with a strong energy shift with increased intensity (peak energy = 1.18 eV at low incident intensity and $k=0.76$ for Eq. (1)). Upon CdCl₂ treatment, the low energy DAP transition is completely quenched while the 1.45 eV A band increases in

intensity. Consonni [15] and Krustok [8] have previously shown the link between the low energy DAP transition and the A band with CdCl₂ treatment, suggesting that the DAP transition is linked to the tellurium vacancy (V_{Te}).

B. Sputtered Thin Film Photoluminescence

While, the as-grown sputtered thin film PL (Fig. 2) differs greatly from the CSS film, *supra vide*, the trends observed upon CdCl₂ treatment are very similar. The as-grown sample has weak emission with no exciton peak at all. The 1.45 eV feature is an overlap of the Y and A bands with no identifiable phonon replica. Krustok et. al [8] observed a single Gaussian 1.08 eV transition, linking it to the sample defect state as the 1.18 DAP. We observe, however, three weak transitions at 1.1 eV, 1.0 eV, and 0.91 eV; for which the source is unclear.

After CdCl₂ treatment, the three low energy transitions are quenched while we see an emergence of the 1.588 (A,X), 1.55 eV (DP), 1.47 eV (Y band) and the 1.457 eV (A band). The exciton peak observed here is consistent with an acceptor-bound exciton which is to be expected after CdCl₂ treatment. The 1.55 eV DP band for the treated sputtered films shows very strong phonon replica. While the 1.47 eV Y band can be identified, it mostly remains swamped out by the very bright 1.45 eV A band.

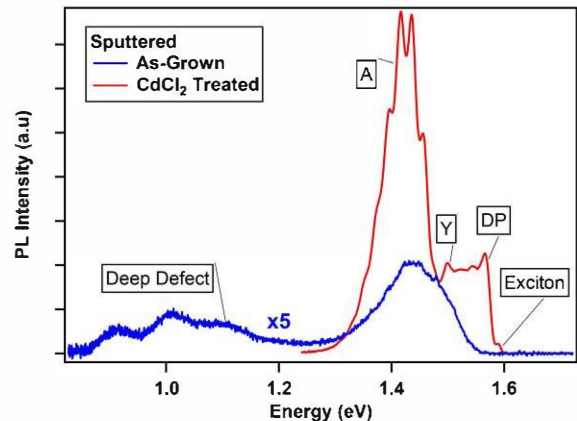


Fig. 2 As-grown (blue curve) and CdCl₂ treated (red curve) CdTe thin films under 1.2 mW/cm² illumination

III. TIME RESOLVED PHOTOLUMINESCENCE

The low energy DAP transition (1.18 eV) presents a unique opportunity to study the lifetime vs donor-acceptor spacing in CdTe, as the PL emission does not strongly overlap with another radiative transition. As such, the remainder of this paper will focus on the deep DAP transition. Utilizing a Fianium SC400-2 WhiteLase ultrafast laser, each sample was excited with 632 nm pulses (5 ps duration) of varying repetition rates ($R_{rep} = 20$ MHz for the 1.59 eV exciton decay; $R_{rep} = 250$ kHz for the other decays). By doing so, we obtain a better understanding of the decay rates of the various radiative recombination pathways. The deep defect states are

longer lived than the measurement capabilities of our system and are fit to a bi-exponential decay profile.

$$y = y_0 + A_1 * \exp\left(\frac{-t}{\tau_1}\right) + A_2 * \exp\left(\frac{-t}{\tau_2}\right) \quad (2)$$

As a result of the low recombination rate, the deep defect states are partially populated when the next laser pulse arrives. As a result, the amplitudes A_1 , A_2 are artificially inflated from their true values and the lifetime parameters τ_1 , τ_2 have larger uncertainties[21], especially when $\tau \gg 1/R_{\text{rep}}$.

The DAP transition (1.1-1.3 eV) of the as-grown CSS sample is of interest for lifetime analysis since the decay has a distance component. Due to Coulomb interaction of the donor/acceptor, the energy of the emitted photon is a function of donor/acceptor separation distance.

$$h\nu = E_G - E_D - E_A + \frac{e^2}{\epsilon r} \quad (3)$$

[22], where E_D and E_A are the donor and acceptor energies with respect to the conduction and valance bands respectively, ϵ is the dielectric constant and e the electron charge. The nearest-neighbor donor acceptor pairs have discrete steps in transition energy while the further pairs blend together (due to smaller increments of distance, r). By selecting the detection wavelength, we probe the effective carrier lifetime of DAP states separated by a small range of distances, $r+dr$; which correlates to the monochromator spectral bandwidth (dE) as:

$$dr = \frac{\epsilon r^2}{e^2} dE \quad (4)$$

The DAP recombination probability varies with r as [22]

$$W(R) = W_{\text{max}} \exp\left[-2r/\alpha_B\right] \quad (5)$$

,where α_B is the Bohr radius of the shallower defect center and W_{max} is the recombination probability of DAPs separated by a large distance where the coulomb interaction is negligible ($r \gg \alpha_B$). Eq. (5) is an approximation for the case when one center (either cation or anion) is shallow and the other is strongly confined. Since it is not clear if this holds true for our DAP recombination, we will utilize the general approach in Section V which is discussed in detail by Novotny,[23] Vink,[24] and Thomas[22] using perturbation theory for dipole transitions of the 1S states. Fig. 3 shows the TRPL decays measured on the high and low energy sides of the DAP pair (1.19 eV peak energy for 1.2 mW/cm² excitation).

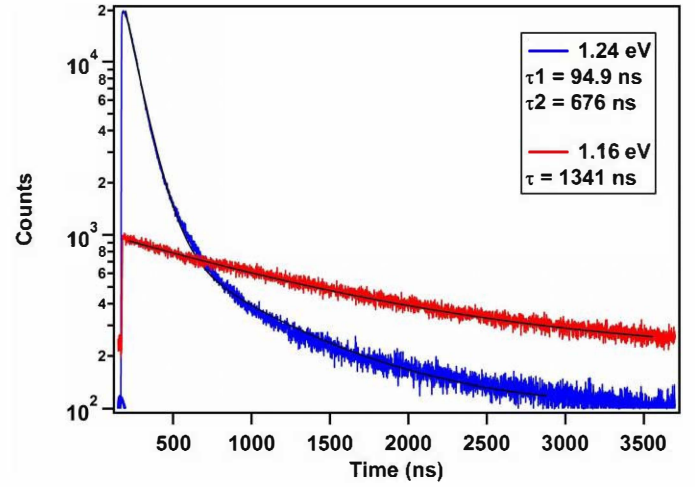


Fig. 3 TRPL decay curves for the CSS sample's DAP transition, measured at the low energy (red curve) and high energy (blue curve) sides of the defect emission under 1.2 mW/cm² excitation [black lines = fit]. The high energy DAP transitions are associated with smaller spacing, Eq. (3), while experiencing a higher recombination probability due to increased overlap of wave functions.

For comparison, Fig. 4 shows TRPL decay profiles for two different energies of the 1.1 eV transition observed in the as-grown sputtered film. Since the carrier recombination rate no does not exhibit a spatial component as does the DAP pair, the carrier lifetime is unchanged when measuring at different energies.

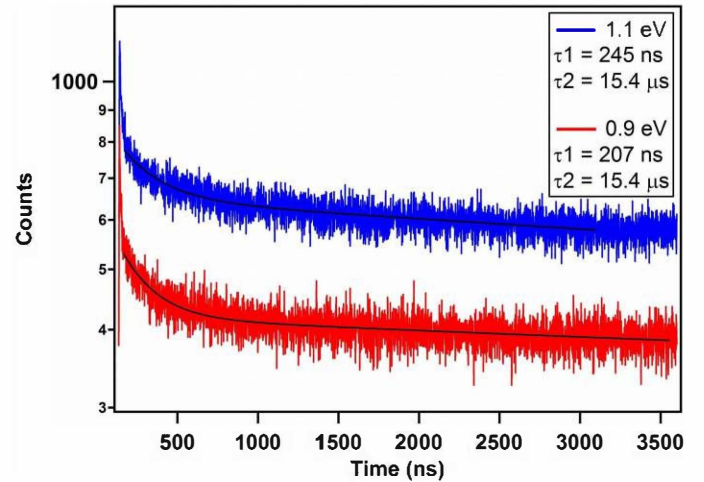


Fig. 4 TRPL decay and fits (black curves) of 1.1 eV peak measured at zero phonon line (blue curve – 1.1 eV) and lower energy phonon line (red curve – 0.9 eV). Extracted lifetimes are very similar within the fit uncertainty.

IV. TIME EVOLUTION OF PHOTOLUMINESCENCE SPECTRA

Compiling the TRPL decay curves, taken at 25 K, as a function of energy, we have constructed PL spectra as a function of time following excitation of a 250 kHz excitation

(incident photon flux of $3.8 \cdot 10^8$ photons/cm²), shown in Fig. 5, for the as-grown CSS CdTe sample. At $t=0.5$ ns, the spectra consists of the Y Band and DAP band. Due to the resolution limit of measuring fast decays on a 4 μ s scale, the high energy side of the spectra has been excluded from this measurement. As time progresses the Y-band quickly decays revealing a lower intensity A band (within less than 100 ns). Since the Y and A band emissions overlap, it is difficult to extract their individual lifetimes, although it is clear that at 3 μ s, the Y band is fully decayed while the A band remains. The initial DAP peak energy of 1.3 eV correlates to a mean pair spacing of approximately 14.5 nm (Eq. (3) using $\epsilon = 10.37$ [25]). As the number of occupied donor/acceptor states decreases the mean spacing $\langle r \rangle$ between pairs increases, thereby decreasing the peak energy of the PL spectra (black arrow in Fig. 5). Beyond 1 μ s, the DAP peak shows little shift in energy with the peak slowly approaching 1.18 eV.

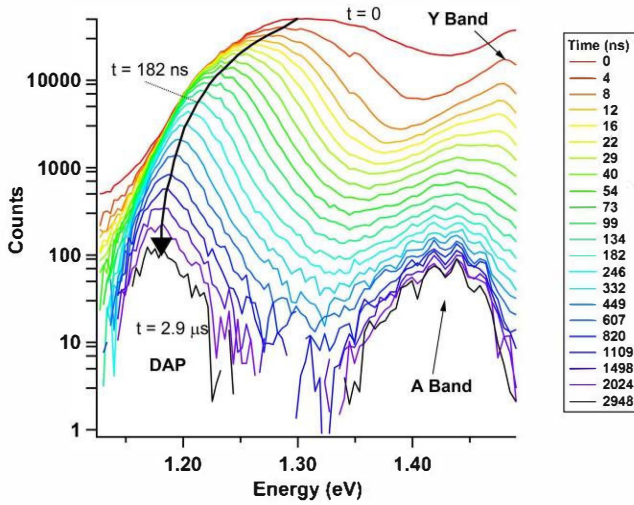


Fig. 5 PL spectra on a semi-log plot of as-grown CSS CdTe at 25 K constructed from TRPL decay curves measured in 3 nm increments. The black arrow traces the DAP peak energy as a function of time. Traces at long time reveal the presence of the A band, which was obscured by the brighter Y band at early delays.

V. CALCULATION OF DONOR ACCEPTOR PAIR RECOMBINATION

As described by Vink [24], the following calculations are performed under the assumption that it is permissible to use the Bohr radii to characterize the wave functions of non-hydrogenic centers using,

$$R_D = \frac{\hbar}{(2m_e^* E_D)^{1/2}}, \quad R_A = \frac{\hbar}{(2m_h^* E_A)^{1/2}} \quad (6)$$

, where m_e^* and m_h^* are the electron and hole effective masses and E_D and E_A are the donor and acceptor ionization energies respectively. The recombination probability for allowed transitions, as a function of r , is given by

$$W(r) = W_{\max} \times |D(r)|^2 \quad (7)$$

$$D(r) = \frac{8(\alpha\beta)^{3/2}}{(\alpha^2 - \beta^2)^3 r} \left\{ [4\alpha\beta + (\alpha^2 - \beta^2)\beta r] \exp(-\alpha r) - [4\alpha\beta - (\alpha^2 - \beta^2)\alpha r] \exp(-\beta r) \right\} \quad (8)$$

, where $\alpha = 1/R_D$ and $\beta = 1/R_A$ and $D(r)$ is related to the interaction of the donor and acceptor wave functions separated by a distance r . Finally, the intensity of light emitted at time t , $I(t)$, is calculated by taking the time derivative of the ensemble average of populated donor/acceptor states $\langle Q(t) \rangle$,

$$\langle Q(t) \rangle = \exp \left[4\pi N \int_0^\infty \{ \exp[-W(r)t] - 1 \} r^2 dr \right] \quad (9)$$

$$I(t) = -\frac{d}{dt} \langle Q(t) \rangle \quad (10)$$

For a first comparison of the observed intensity decay to theory, we utilize the energy levels proposed by Krustok et. al [8] of $E_D = 0.317$ eV and $E_A = 0.113$ eV. Using Eq. (6) with effective mass values of $m_h^* = 0.35m_0$ and $m_e^* = 0.096m_0$ [26] we obtain Bohr radii values of $R_D = 11.16$ Å and $R_A = 9.78$ Å. Allowing W_{\max} and N (majority defect concentration) to vary, we find the closest fit for $W_{\max} = 4.9 \cdot 10^8$ s⁻¹ and $N = 2.5 \cdot 10^{17}$ cm⁻³, see Fig. 6.

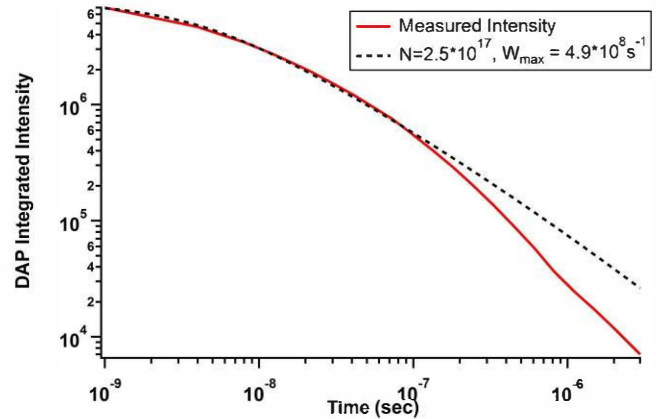


Fig. 6 Log-log plot of DAP integrated intensity (red curve), from Fig. 5, along with the calculated decay using Eq. (10) (black dotted curve).

VI. SUMMARY

Low temperature PL measurements show (Figs. 1 and 2) different intrinsic defects (as-grown) for CSS and sputtered depositions. After CdCl₂ treatment, the CSS and sputtered

films show the same defect transitions with varying intensities (likely due to different final defect concentrations). TRPL measurements of the lowest energy states in the as-grown films (1.18 eV for CSS and 1.1 eV for sputtered) show the direct observation of increased carrier recombination rate for DAPs with decreasing separation Eq. (5). Time dependent PL spectra (Fig. 5) reconstructed from TRPL curves show the energy shift of the DAP transition with the increasing mean spacing $\langle r \rangle$ over time. Additionally, the long time plots reveal the presence of the A band for the as-grown CSS sample, which was not obvious in the steady-state PL spectra.

ACKNOWLEDGEMENT

P.R. and R.E. were supported by the Air Force Research Laboratory under contracts F9453-08-C-0172 and F9453-11-C-0253. N.P. and Y.Y. were supported by the U.S. DOE F-PACE Program and the National Science Foundation's Sustainable Energy Pathways Program under contract CHE-1230246. C. X. was supported by the University of Toledo, College of Natural Sciences and Mathematics, School for Solar and Advanced Renewable Energy (SSARE). The authors gratefully acknowledge Richard K. Ahrenkiel for helpful discussion of CdTe photoluminescence, including insight regarding signatures of the DAP transition.

REFERENCES

- [1] M. A. Green, *et al.*, "Solar cell efficiency tables (version 43)," *Progress in Photovoltaics: Research and Applications*, vol. 22, pp. 1-9, 2014.
- [2] First Solar Inc. (2014, Accessed May 26, 2014). *First Solar Sets World Record for CdTe Solar Cell Efficiency*. Available: <http://investor.firstsolar.com/releasedetail.cfm?ReleaseID=828273>
- [3] N. R. Paudel, *et al.*, "Post-deposition processing options for high-efficiency sputtered CdS/CdTe solar cells," *Journal of Applied Physics*, vol. 115, pp. -, 2014.
- [4] H. R. Moutinho, *et al.*, "Investigation of polycrystalline CdTe thin films deposited by physical vapor deposition, close-spaced sublimation, and sputtering," *Journal of Vacuum Science & Technology A*, vol. 13, pp. 2877-2883, 1995.
- [5] D. M. Hofmann, *et al.*, "Identification of the chlorine A center in CdTe," *Physical Review B*, vol. 45, pp. 6247-6250, 1992.
- [6] S. Seto, *et al.*, "Chlorine-related photoluminescence lines in high-resistivity Cl-doped CdTe," *Journal of crystal growth*, vol. 117, pp. 271-275, 1992.
- [7] A. V. Kvit, *et al.*, "Characterization of the Z luminescence system in high purity CdTe," *Materials Science and Engineering: B*, vol. 26, pp. 1-5, 1994.
- [8] J. Krustok, *et al.*, "Deep center luminescence in p-type CdTe," *Journal of Applied Physics*, vol. 80, pp. 1757-1762, 1996.
- [9] D. Halliday, *et al.*, "A photoluminescence study of polycrystalline thin-film CdTe/CdS solar cells," *Journal of crystal growth*, vol. 186, pp. 543-549, 1998.
- [10] J. Krustok, *et al.*, "Photoluminescence Properties of Z-Bands in CdTe," *physica status solidi (a)*, vol. 165, pp. 517-525, 1998.
- [11] D. Grecu, *et al.*, "Photoluminescence of Cu-doped CdTe and related stability issues in CdS/CdTe solar cells," *Journal of Applied Physics*, vol. 88, pp. 2490-2496, 2000.
- [12] J. Aguilar-Hernández, *et al.*, "Analysis of the 1.55 eV PL band of CdTe polycrystalline films," *Materials Science and Engineering: B*, vol. 102, pp. 203-206, 2003.
- [13] C. R. Corwine, *et al.*, "CdTe photoluminescence: Comparison of solar-cell material with surface-modified single crystals," *Applied Physics Letters*, vol. 86, pp. -, 2005.
- [14] J. Van Gheluwe, *et al.*, "Photoluminescence study of polycrystalline CdS/CdTe thin film solar cells," *Thin Solid Films*, vol. 480-481, pp. 264-268, 2005.
- [15] V. Consonni, *et al.*, "Spectroscopic analysis of defects in chlorine doped polycrystalline CdTe," *Journal of Applied Physics*, vol. 99, pp. -, 2006.
- [16] N. Armani, *et al.*, "Role of thermal treatment on the luminescence properties of CdTe thin films for photovoltaic applications," *Thin Solid Films*, vol. 515, pp. 6184-6187, 2007.
- [17] S. Vatavu, *et al.*, "Photoluminescence studies of CdTe films and junctions," *Thin Solid Films*, vol. 515, pp. 6107-6111, 2007.
- [18] C. Kraft, *et al.*, "Comprehensive photoluminescence study of chlorine activated polycrystalline cadmium telluride layers," *Journal of Applied Physics*, vol. 108, pp. -, 2010.
- [19] N. R. Paudel and Y. Yan, "Fabrication and characterization of high-efficiency CdTe-based thin-film solar cells on commercial SnO₂:F-coated soda-lime glass substrates," *Thin Solid Films*, vol. 549, pp. 30-35, 2013.
- [20] N. R. Paudel, *et al.*, "Ultrathin CdS/CdTe solar cells by sputtering," *Solar Energy Materials and Solar Cells*, vol. 105, pp. 109-112, 2012.
- [21] R. W. K. Leung, *et al.*, "Effects of incomplete decay in fluorescence lifetime estimation," *Biomedical Optics Express*, vol. 2, pp. 2517-2531, 2011/09/01 2011.

- [22] D. G. Thomas, *et al.*, "Kinetics of Radiative Recombination at Randomly Distributed Donors and Acceptors," *Physical Review*, vol. 140, pp. A202-A220, 1965.
- [23] V. Novotny, "Radiative recombination rate of donor-acceptor pairs," *Canadian Journal of Physics*, vol. 47, pp. 1971-1977, 1969/09/15 1969.
- [24] A. T. Vink, "The dependence of the radiative transition probability of donor-acceptor pairs on pair separation," *Journal of Luminescence*, vol. 9, pp. 159-179, 1974.
- [25] I. Strzalkowski, *et al.*, "Dielectric constant and its temperature dependence for GaAs, CdTe, and ZnSe," *Applied Physics Letters*, vol. 28, pp. 350-352, 1976.
- [26] R. Triboulet and P. Siffert, *CdTe and Related Compounds; Physics, Defects, Hetero- and Nanostructures, Crystal Growth, Surfaces and Applications: Physics, CdTe-based Nanostructures, CdTe-based Semimagnetic Semiconductors, Defects*: Elsevier Science, pp. 61, 2009.